Neurobiology of Aging 50 (2017) 87–95

Contents lists available at ScienceDirect

Neurobiology of Aging

journal homepage: www.elsevier.com/locate/neuaging

Age-related differences in the structural complexity of subcortical and ventricular structures

Christopher R. Madan*, Elizabeth A. Kensinger

Department of Psychology, Boston College, Chestnut Hill, MA, USA

ARTICLE INFO

Article history:
Received 5 September 2016
Received in revised form 19 October 2016
Accepted 20 October 2016
Available online 27 October 2016

Keywords:
Brain morphometry
Age
Atrophy
Fractal dimensionality
Thalamus
Hippocampus
Putamen
Ventricles

ABSTRACT

It has been well established that the volume of several subcortical structures decreases in relation to age. Different metrics of cortical structure (e.g., volume, thickness, surface area, and gyrification) have been shown to index distinct characteristics of interindividual differences; thus, it is important to consider the relation of age to multiple structural measures. Here, we compare age-related differences in subcortical and ventricular volume to those differences revealed with a measure of structural complexity, quantified as fractal dimensionality. Across 3 large data sets, totaling nearly 900 individuals across the adult lifespan (aged 18–94 years), we found greater age-related differences in complexity than volume for the subcortical structures, particularly in the caudate and thalamus. The structural complexity of ventricular structures was not more strongly related to age than volume. These results demonstrate that considering shape-related characteristics improves sensitivity to detect age-related differences in subcortical structures.

1. Introduction

The structure of the brain changes with age, and these changes can be measured in vivo using magnetic resonance imaging (MRI) (Creasey and Rapoport, 1985; Drayer, 1988; Kemper, 1994; Raz and Rodrigue, 2006). Although age-related differences are apparent throughout the brain, differences are particularly evident in the volume of subcortical structures (Allen et al., 2005; Goodro et al., 2012; Greenberg et al., 2008; Gunning-Dixon et al., 1998; Inano et al., 2013; Jernigan et al., 2001; Long et al., 2012; Potvin et al., 2016; Raz et al., 2004, 2005; Tamnes et al., 2013; Walhovd et al., 2005, 2011; Yang et al., 2016). Accompanying these changes, the ventricles also enlarge with age (Apostolova et al., 2012; Barron et al., 1976; Kaye et al., 1992; LeMay, 1984; Nestor et al., 2008; Walhovd et al., 2011). Here, we investigated age-related changes in the shape of these same subcortical structures and tested if this additional information could explain variance beyond that explained by volumetric changes.

Walhovd et al. (2011) conducted a comprehensive review of the literature examining age-related differences in subcortical structures. In their review, along with their own multisample analyses, they found strong age-related differences in the volume of the putamen, thalamus, and accumbens; other regions, including the caudate and amygdala, were relatively unaffected by aging. Walhovd et al. also found volumetric differences in the lateral ventricles and third ventricle to also be strongly related to age, but no age-related differences in the fourth ventricle. In a supplemental figure (Walhovd et al., 2011, Figure S2), the authors additionally illustrated age differences in the shape of these subcortical structures, though there was no accompanying quantitative analysis of shape.

Although it is known that there are age-related differences in cortical thickness and gyrification (Fjell et al., 2009; Hogstrom et al., 2013; McKay et al., 2014; Salat et al., 2004), many other morphologic measures can also be examined (e.g., sulcal depth, span, and variability [Im et al., 2006; Kochunov et al., 2008; Thompson et al., 1996; Yun et al., 2013]; curvature [Fischl et al., 1999; Pienaar et al., 2008]). Recently, we demonstrated that age-related differences in the shape, that is, structural complexity, of cortical regions were more pronounced than in cortical thickness or gyrification (Madan and Kensinger, 2016). Moreover, we found that complexity statistically accounted for all the age-related differences associated with cortical thickness and gyrification. Although it is currently unclear what features of brain morphology are captured by this metric of complexity, the results underscore that—at least for cortical regions—complexity

* Corresponding author at: Department of Psychology, Boston College, McGuinn 300, 140 Commonwealth Ave., Chestnut Hill, MA 02467, USA. Tel.: +1-617-552-2231; fax: +1-617-552-0523.
E-mail address: madanc@bc.edu (C.R. Madan).

0197-4580/$ – see front matter © 2016 Elsevier Inc. All rights reserved.
http://dx.doi.org/10.1016/j.neurobiolaging.2016.10.023

is a particularly robust metric for assessing age-associated differences. Of course, explaining the "most" age-related variability is not always desired, as this may leave less remaining variance to account for other sources of interindividual variability (e.g., cognitive abilities); but the extant research suggests that if the goal is to estimate effects of age on brain morphology, metrics of structural complexity may be of particular utility.

Here, we sought to extend this research by assessing the extent by which complexity can improve the characterization of age-related differences in brain structure beyond the cortex, by examining subcortical and ventricular structures. A number of studies have demonstrated that the shape of subcortical structures can differ between patients and healthy controls. For instance, autism has been associated with differences in the shape of the amygdala (Chung et al., 2008), Alzheimer's disease has been related to differences in several structures, particularly the hippocampus, amygdala, and lateral ventricles (Tang et al., 2014), and schizophrenic patients have shown differences in hippocampal and thalamus shape (Zhao et al., 2016; also see Smith et al., 2011 and Qiu et al., 2009). Although these studies provide evidence that shape characteristics can be a relevant measure for subcortical structures, it is possible that these systematic differences only occur in the presence of neurological or psychiatric disorders. Furthermore, increased explained variance may not always be desired, instead, we propose that the use of multiple metrics can lead to better characterization of interindividual differences.

Here, we used fractal dimensionality to measure the structural complexity of the investigated subcortical and ventricular structures. This approach was inspired by the innovative work of Mandelbrot (1967), where fractal geometry principles were applied to quantify the complexity of complex natural structures. Although Mandelbrot initially applied fractal dimensionality to geographic data (coast lines), neuroimagers have previously considered the notion of using fractal dimensionality to quantify the complexity of the brain (e.g., Free et al., 1996; Hofman, 1991; Kiselev et al., 2003). More broadly, fractal dimensionality has been used in neuroscience from the scale of individual neurons to the whole brain (see Di Ieva et al., 2013, 2015, for a review).

Using 3 large data sets, here we first replicated the age-related differences in volume of subcortical and ventricular structures, then further calculated age-related differences in their structural complexity. The present study addressed 2 primary questions: (1) are there systematic age-related differences in the shape of subcortical structures, as indexed by structural complexity, using the same approach as in Madan and Kensinger (2016); and (2) how do these differences compare to volumetric age-related differences in these structures. Different structural measures may also serve complimentary roles—where different measures may index distinct population-level characteristics; as such we additionally assessed the collinearity of the measures and the unique variance they can explain with respect to age-related variability.

2. Procedure

2.1. Data sets

Three data sets were used to evaluate age-related differences in subcortical and ventricular structure.

Sample 1 (OASIS) consisted of 314 healthy adults (196 females), aged 18–94 years, from the publicly available Open Access Series of Imaging Studies (OASIS) cross-sectional data set (Marcus et al., 2007; http://www.oasis-brains.org). Participants were recruited from a database of individuals who had (1) previously participated in MRI studies at Washington University; (2) were part of the Washington University Comminity; or (3) were from the longitudinal pool of the Washington University Alzheimer Disease Research Center. Participants were screened for neurological and psychiatric issues; the Mini-Mental State Examination (MMSE) and Clinical Dementia Rating were administered to participants aged 60 and older. In the current sample, participants with a Clinical Dementia Rating above zero were excluded; all remaining participants scored 25 or above on the MMSE. Multiple T_1 volumes were acquired using a Siemens Vision 1.5 T with an MPRAGE sequence; only the first volume was used here. Scan parameters were: repetition time = 9.7 ms; echo time = 4.0 ms; flip angle = 10°; voxel size = 1.25 × 1 × 1 mm.

Sample 2 (IXI) consisted of 427 healthy adults (260 females), aged 20–86, from the publicly available Information eXtraction from Images (IXI) data set (http://brain-development.org/ixi-dataset/). This is the same set of individuals we used previously to investigate age-related differences in the cortex (Madan and Kensinger, 2016). These individuals were scanned at 1 of 3 hospitals in the London, UK (Guy's Hospital, Hammersmith Hospital, and Institute of Psychiatry) in 2005–2006. Details on how these individuals were recruited is unavailable nor are details on how mental health was assessed. See Madan and Kensinger (2016) for further details.

Sample 3 (BC) consisted of 176 healthy adults (89 females), aged 18–83 years, recruited by the Cognitive and Affective Laboratory at Boston College (BC) in 2012–2015. All participants were screened for neurological and psychiatric issues and to have scored above 26 on the MMSE. T_1 volumes were acquired using a Siemens Trio 3 T with an MEMPRAGE sequence optimized for morphometry studies (van der Kouwe et al., 2008; Wonderlick et al., 2009). Scan parameters were: TR = 2530 ms; TE = 1.64, 3.50, 5.36, and 7.22 ms; flip angle = 7°; voxel size = 1 × 1 × 1 mm.

2.2. Segmentation and volumetric analyses

All structural MRIs were processed using FreeSurfer 5.3.0 on a machine running CentOS 6.6 (Fischl, 2012; Fischl and Dale, 2000; Fischl et al., 2002). FreeSurfer's standard pipeline was used (i.e., recon-all). FreeSurfer's segmentation procedure produces labels for 7 subcortical structures (thalamus, hippocampus, amygdala, caudate, putamen, accumbens, and palladium) and 4 ventricular structures (lateral, inferior lateral, third, and fourth) all within a common segmentation volume (Fischl et al., 2002, 2004). Fig. 1 shows the subcortical structures investigated here. Volumes for subcortical and ventricular structures were obtained directly from FreeSurfer.

Validation studies have shown that this automated segmentation procedure corresponds well with manual tracing (e.g., Fischl et al., 2002; Jovicich et al., 2009; Keller et al., 2012; Lehmann et al., 2010; Mulder et al., 2014; Pardoe et al., 2009; Tae et al., 2008; Wenger et al., 2014). FreeSurfer has been used in a large number of studies investigating age differences in subcortical structures (e.g., Inano et al., 2012; Jovicich et al., 2009; Long et al., 2012; Potvin et al., 2016; Tamnes et al., 2013; Walhovd et al., 2005, 2011; Wenger et al., 2014; Yang et al., 2016).

Intracranial volume (ICV) was also estimated using FreeSurfer (Buckner et al., 2004), which has also been shown to correspond well with manual tracing (Sargolzaei et al., 2015).

2.3. Fractal dimensionality analyses

The complexity of each structure was calculated using the calcFD toolbox (Madan and Kensinger, 2016; http://cmadan.github.io/calcFD/). This toolbox calculates the "fractal dimensionality" of a 3D structure and is specifically designed to use intermediate files

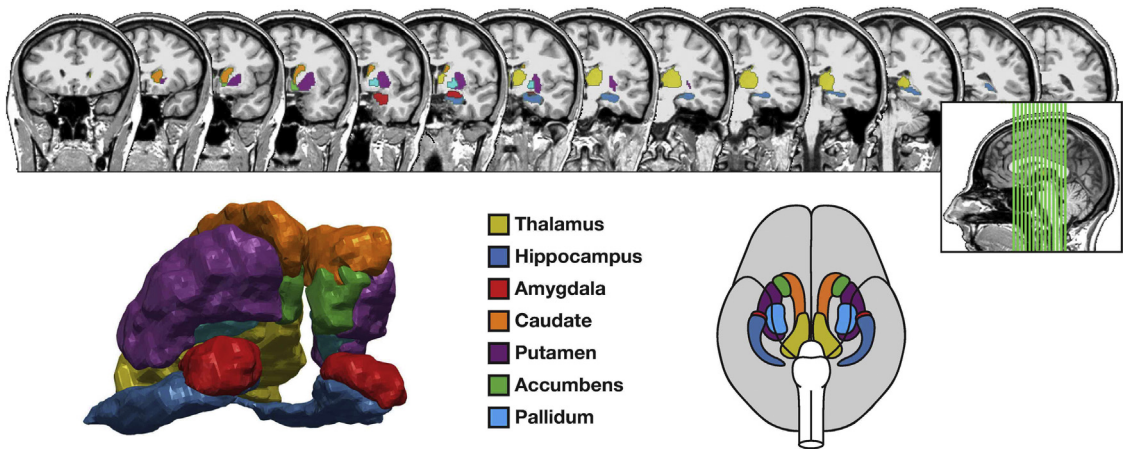

Fig. 1. Coronal slices, 3D reconstruction, and 2D illustration of the 7 subcortical structures examined. Coronal slices, with anterior slices on the left, are shown at 5-mm spacing from a representative participant; positions of the displayed coronal slices are marked on the inset sagittal slice. The 3D reconstruction is based on the same participant's MRI as the coronal slices (following from Madan, 2015). The 2D illustration was adapted from Toro et al. (2014).

from the standard FreeSurfer analysis pipeline, here aparc.a2009s+aseg.mgz. The toolbox has previously been used with parcelated cortical structure, as well as validated using several benchmark volumes (Madan and Kensinger, 2016).

We use fractal dimensionality as a measure of the complexity of a 3D structure, that is, a subcortical structure. Unlike volume, which corresponds to the "size" of any 3D structure, fractal dimensionality measures shape information and is scale invariant (Madan and Kensinger, 2016).

In fractal geometry, several approaches have been proposed to quantify the "dimensionality" or complexity of a fractal; the approach here calculates the Minkowski–Bouligand or Hausdorff dimension (see Mandelbrot, 1967). This structural property can be measured by considering the 3D structure within a grid space and counting the number of boxes that overlap with the edge of the structure, referred to as the "box-counting algorithm" (Caserta et al., 1995; Mandelbrot, 1982). By then using another grid size (i.e., changing the box width), the relationship between the grid size and number of counted boxes can be determined. Here, we used box sizes (in mm) corresponding to powers of 2, ranging from 0 to 4 (i.e., 2^k [$k = 0, 1, 2, 3, 4$] = 1, 2, 4, 8, 16 mm). The slope of this relationship in log-log space is the fractal dimensionality of the structure. Thus, the corresponding equation is:

$$FD = -\frac{\Delta \log_2(\text{Count})}{\Delta \log_2(\text{Size})}$$

There are 2 distinct fractal dimensionality values that can be calculated: If only the boxes overlapping with the edge/surface of the structure are counted, this slope represents the fractal dimensionality of the surface, denoted as FD_s. If the boxes within the structure are also counted, the resulting slope represents the fractal dimensionality of the filled volume, denoted as FD_f.

As the relative alignment of the grid space and the structure can influence the obtained fractal dimensionality value using the box-counting algorithm, we instead used a dilation algorithm that is equivalent to using a sliding grid space and calculating the fractal dimensionality at each alignment (Madan and Kensinger, 2016) but can be calculated much faster as it is less computationally demanding. This was implemented using a 3D-convolution operation (convn in MATLAB). As an example, Fig. 2 illustrates the calculation of fractal dimensionality for a complex 2D structure.

2.4. Data analysis

All volume measurements were ICV-corrected before conducting the regression analyses. Specifically, ICV-corrected volumes were calculated as the residual after the volume data was regressed for ICV (as in Walhovd et al., 2011). Formal comparisons of procedures used to adjust for ICV suggest that results generalize across differing procedures (Greenberg et al., 2008).

Age differences in the subcortical and ventricular structures were first assessed using regression models examining the linear and quadratic relationships between age and volume (or fractal dimensionality) of the structure, with the amount of variance explained (i.e., R^2) as the statistic. All of the regression models reported controlled for effects of sex (and site, in the case of the IXI data set).

To directly assess if fractal dimensionality explained more age-related variability than volume, we formally compared model fits based on either measure, for each structure, using the Bayesian Information Criterion (BIC). This approach allows us to compare different regression models and determine which model fits the data best, or if models perform comparably. In addition, models with more parameters are penalized for these additional degrees of freedom. As a rule of thumb, if the difference in BIC between 2 models is less than 2, neither of the models' fit to the data is significantly better (Burnham and Anderson, 2002, 2004). As absolute BIC values are arbitrary, we subtract the BIC value for the best model considered from all BIC values and report ΔBIC for each of the models, as is common practice. As a result, the best model considered is ΔBIC = 0.00 by definition.

3. Results

3.1. Age-related differences in subcortical structures

We used the OASIS data set as our primary sample because Walhovd et al. (2011) previously examined age-related differences in volumetric measures in this sample (samples 4a and 4b in their analyses). As such, the volumetric analyses here were intended to serve as a replication of their findings.

The subcortical structures investigated here were the thalamus, hippocampus, amygdala, caudate, putamen, accumbens, and pallidum; a representative reconstruction of the structures from a participant's MRI is shown in Fig. 1. As shown in Table 1, linear and

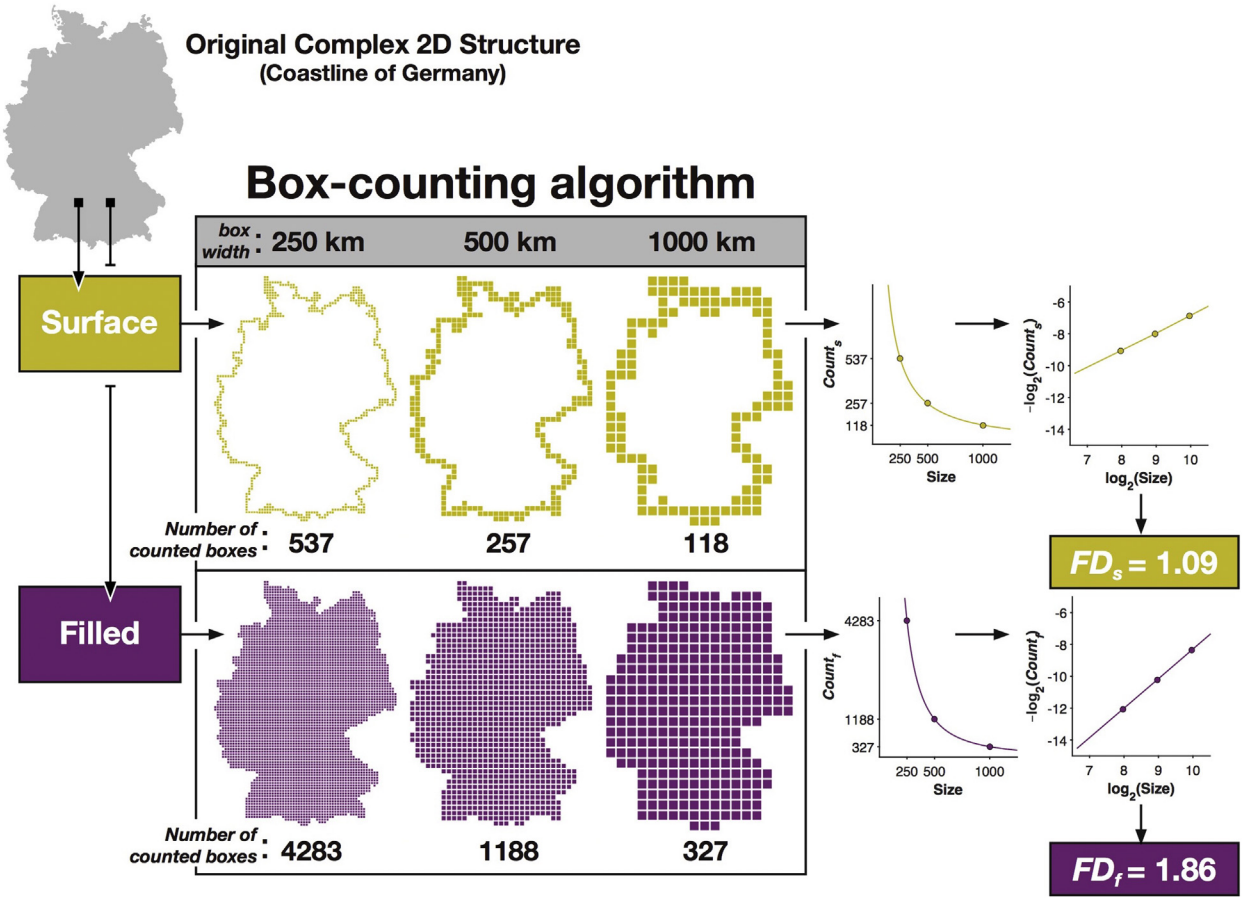

Fig. 2. Illustration of how fractal dimensionality is measured from a 2D structure. Reprinted from Madan and Kensinger (2016) with permission. Copyright 2016, Elsevier.

quadratic relationships between age and volumes of subcortical structures closely matched the amount of variance explained (i.e., R^2) reported by Walhovd et al. (2011) for the same sample. Briefly, age-related differences were most pronounced in the thalamus, putamen, accumbens, and pallidum—each with R^2 values near 50% or above (Fig. 3A). Age explained a moderate amount of variability in the volume of the hippocampus and amygdala, whereas caudate volume was the least related to age-related differences. The upper half of Fig. 4 shows the quadratic fits for each structure.

We calculated the fractal dimensionality, both FD_s and FD_f, of the structures for each individual to additionally measure age-related differences in their structural complexity. Fractal dimensionality of the surface (FD_s) captured more variability than volume for some

Table 1
Effects of age on volume and fractal dimensionality for the structures examined

Structure	Volume						FD_f					
	1		2		3		1		2		3	
	OASIS		IXI		BC		OASIS		IXI		BC	
	Age	Age^2	Age	Age^2	Age	Age^2	Age	Age^2	Age	Age^2	Age	Age^2
Thalamus	**0.55**	*0.55*	**0.28**	**0.30**	**0.28**	**0.37**	**0.71**	**0.74**	**0.52**	**0.54**	**0.51**	**0.56**
Hippocampus	**0.26**	**0.38**	**0.14**	**0.20**	**0.38**	**0.47**	**0.31**	**0.43**	**0.10**	**0.13**	**0.26**	**0.32**
Amygdala	**0.18**	**0.21**	**0.10**	**0.12**	**0.35**	**0.42**	**0.28**	**0.33**	**0.23**	*0.24*	**0.42**	**0.48**
Caudate	**0.03**	**0.12**	**0.05**	0.06	**0.04**	**0.10**	**0.39**	*0.40*	**0.26**	0.26	**0.29**	*0.31*
Putamen	**0.51**	0.51	**0.28**	0.28	**0.50**	*0.51*	**0.62**	0.62	**0.32**	0.32	**0.44**	**0.46**
Accumbens	**0.53**	**0.54**	**0.23**	0.23	**0.44**	0.45	**0.61**	**0.65**	**0.31**	0.31	**0.47**	*0.49*
Pallidum	**0.47**	0.48	**0.06**	0.06	**0.33**	0.34	**0.49**	0.49	**0.10**	0.11	**0.30**	0.31
Ventricles												
Lateral	**0.53**	**0.60**	**0.32**	**0.38**	**0.44**	**0.48**	**0.51**	**0.53**	**0.26**	**0.28**	**0.48**	0.48
Inferior lateral	**0.39**	**0.57**	**0.19**	**0.28**	**0.28**	**0.32**	**0.30**	**0.41**	**0.07**	**0.09**	**0.25**	*0.28*
3rd	**0.52**	**0.63**	**0.30**	**0.34**	**0.44**	**0.49**	**0.52**	**0.59**	**0.28**	**0.30**	**0.43**	**0.47**
4th	**0.02**	**0.08**	0.01	*0.02*	0.00	0.00	0.00	**0.08**	0.00	*0.01*	0.01	0.01

Volume measures were ICV-corrected; effects of site were regressed out for the IXI sample. Values in the Age^2 columns indicate amount of explained variance (R^2) for the model consisting of Age + Age^2 and are printed in bold/italic + underline only if the addition of the quadratic term significantly increased the amount of explained variance. Bold: $p < 0.01$; italic + underline: $p < 0.05$.
Key: BC, Boston College; ICV, intracranial volume; IXI, Information eXtraction from Images; OASIS, Open Access Series of Imaging Studies.

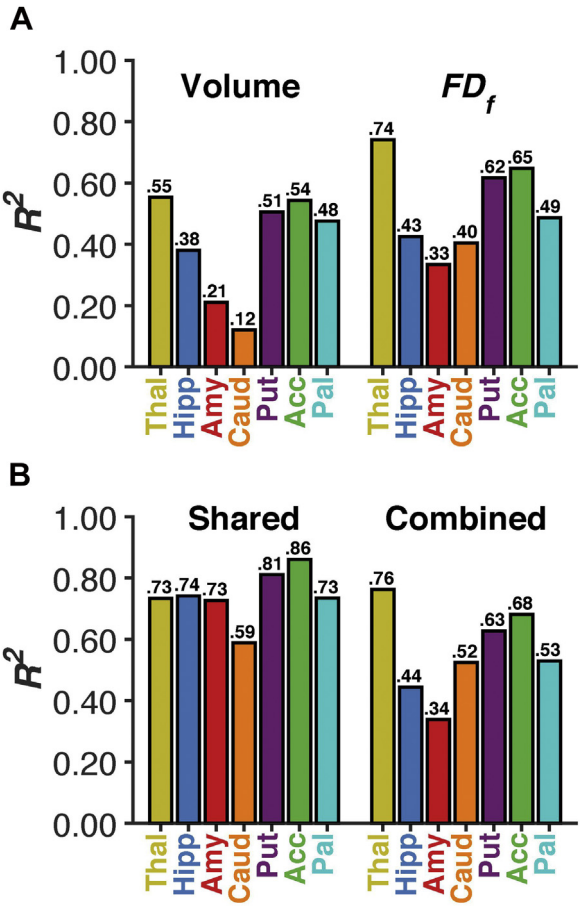

Fig. 3. Amount of variance explained (R^2) by quadratic models of age in volume and structural complexity for each subcortical structure (A). (B) The panel represents amount of variance common to both volume and complexity (i.e., collinearity), as well as combined variance explained by including both volume and complexity.

of the structures; for instance, 64% for the thalamus and 66% for the accumbens. There was a smaller increase in variability explained by FD_s relative to volume in the amygdala (31%), and there was effectively no additional age-related differences explained in the caudate (16%). However, less variability was explained by FD_s than by volume in other structures, such as the hippocampus (20%), putamen (31%), and pallidum (36%). Importantly, FD_s captures shape-related, but not volumetric, characteristics of the surface structure. In contrast, FD_f, while scale invariant, is influenced by a combination of shape- and volumetric-related characteristics of the structure. Age-related differences in FD_f were larger than those for volume across all 7 subcortical structures, as shown in Table 1 and Fig. 3A; differences were also larger than for FD_s for all but 1 structure, although that comparison was only nominally smaller (accumbens, quadratic R^2: FD_s = 66%; FD_f = 65%). Relative to volume, the amount of variability explained in FD_f was much higher for the thalamus and caudate (74% and 40% variance explained with the quadratic model, respectively; vs. 55% and 12% with volume, respectively). More moderate increases (of approximately 10% more variance explained) were found for the amygdala, putamen, and accumbens. The lower half of Fig. 4 shows the quadratic fits for the structures; relationships are generally consistent as those with volume, although generally there is less unexplained variability (i.e., the residual).

Fig. 3B illustrates that volume and structural complexity are highly collinear. Volume and structural complexity were the most distinct for the caudate, with 59% shared variance. Apart from the caudate, the amount of shared variance ranged from 73%–86%. Including both volume and structural complexity within the same model marginally increased the total amount of variance explained (Fig. 3B) relative to the FD_f models, with increases ranging from 1%–4% for 6 of the structures. However, the inclusion of volume led to a 12% additional variance explained for the caudate, suggesting that age-related differences in volume and complexity were distinct for this region.

The 2 fractal dimensionality measures were slightly more collinear, with shared variances of thalamus (77%), hippocampus (71%), amygdala (85%), caudate (76%), putamen (63%), accumbens (99%), and pallidum (72%). In almost all cases, the combined variance explained by the 2 fractal dimensionality measures was increased by less than 5% relative to the FD_f-only regression model; the only exception to this was the caudate, where the combined model explained 56% of age-related variability.

Formal model comparisons are reported in Table 2. In contrast to the analyses presented in Figs. 3 and 4 and Table 1, in which the structural measures were used as the dependant variable (DV), here we used age as the DV such that we could compare how well the various structural measures were able to explain variability in this common DV. Here, we found that fractal dimensionality explained more age-related variability than volume for all of the subcortical structures.

3.2. Limitations to scale invariance of fractal dimensionality

Although fractal dimensionality is mathematically scale invariant, constraints of MRI data acquisition may introduce a lower limit to this theoretical property. Specifically, smaller structures are inherently more “rectangular” due to voxel resolution constraints

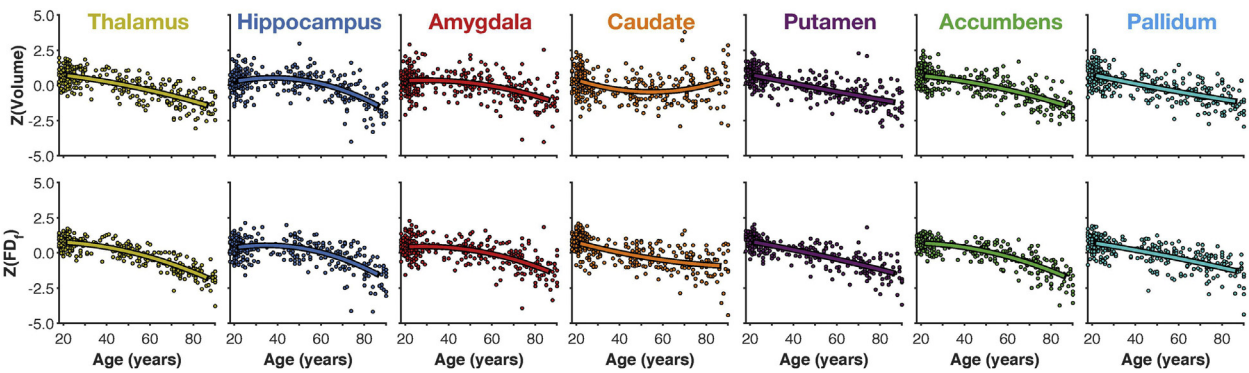

Fig. 4. Scatter plots of age-related differences in volume and structural complexity for each subcortical structure along with best-fitting quadratic models.

Table 2
Model fitness in comparing the effects of volume and fractal dimensionality in explaining age, for each of the structures examined, based on the OASIS data set

Structure	Volume		FD_f	
	Linear	Quadratic	Linear	Quadratic
Thalamus	138.81	144.04	**0.00**	**1.97**
Hippocampus	294.06	292.48	**268.43**	274.18
Amygdala	325.39	328.65	**282.02**	285.23
Caudate	378.02	374.80	**230.20**	234.18
Putamen	166.08	166.43	**87.17**	91.08
Accumbens	148.45	146.21	88.52	**85.10**
Pallidum	185.06	188.54	**178.19**	**177.54**
Ventricles				
Lateral	151.21	**111.27**	160.55	148.52
Inferior lateral	229.71	**212.61**	274.11	260.23
3rd	156.98	**123.98**	154.28	144.76
4th	**380.47**	385.83	386.21	387.84

Values in the quadratic columns indicate model fitness (ΔBIC) for the regression model consisting of both linear and quadratic terms. Models with BIC values with a difference greater than 2 suggest that the model with the lower BIC value is a significantly better fit than the other models. Best fitting models for each structure are denoted in bold.

and thus will have lower structural complexity as a result. A lower limit on the scale invariance of fractal dimensionality would appear as a steep relationship with volume, indicating that the resolution of the 3D structure's shape was insufficient to yield additional contributions from shape-related properties.

Here, we examined the relationship between total volume (without ICV-correction) and FD_f and found some evidence of a limitation in scale invariance (Fig. 5). Specifically, smaller subcortical structures (e.g., accumbens, pallidum) had steeper relationships between volume and FD_f and less "off-axis" variability than larger structures (e.g., thalamus, caudate). This indicates that (1) FD_f for smaller structures was influenced more by volumetric characteristics than in the larger structures; and (2) FD_f for smaller structures was more correlated with volume, whereas FD_f for larger structures additionally indexed other sources of variability (i.e., shape-related characteristics). This increase in off-axis variability was not true of all larger structures, specifically the putamen, although this could be related to biological constraints in the variability in shape of the structure.

These results indicate that future applications of structural complexity will be limited for structures that are inherently small (e.g., hippocampal subfields), although this limitation can be attenuated by acquiring MRI data with higher-resolution imaging protocols (i.e., decreasing the voxel size during acquisition). As noted in the Methods section, the MRI data in the data sets analyzed here were acquired with a voxel size of 1 mm 3-isotropic or slightly larger. However, when anatomical fidelity is critical, current neuroimaging protocols can acquire high-resolution images with voxel dimensions on the scale of 0.5-mm in-plane (e.g., Hrybouski et al., 2016; La Joie et al., 2010; Palombo et al., 2013; Reagh and Yassa, 2014; Yushkevich et al., 2015).

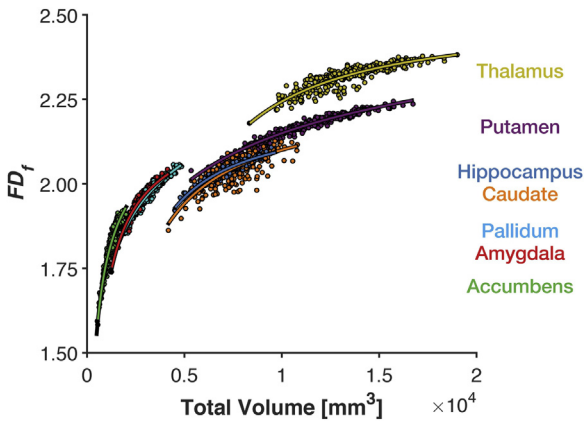

Fig. 5. Scatter plot of total volume and structural complexity along with best-fitting power-function models.

3.3. Age-related differences in the ventricles

We also examined age-related differences in the volume and structural complexity of the ventricles, as shown in Fig. 6. The amount of variability in volume explained by age-related differences was consistent with Walhovd et al. (2011). Interestingly, variability in the fractal dimensionality (FD_f) of the structures was more weakly associated with age-related differences than volume, unlike the subcortical structures (see Table 1). When formally compared (see in the following sections), volume explained more age-related variability than fractal dimensionality for all of the ventricular structures (Table 2).

3.4. Replication in independent samples

To assess the reproducibility of our findings of age-related differences in the structural complexity of the subcortical and ventricular structures, we conducted similar analyses in 2 additional samples.

In the IXI sample, we generally found less age-related differences in both volume and fractal dimensionality; however, the volumetric differences observed here were within the intersample variability observed in Walhovd et al. (2011). Importantly, the same regions were found to show the strongest age-related differences in volume (e.g., thalamus, putamen, and lateral ventricles; although not the pallidum). Fractal dimensionality (FD_f) was again more closely related to age-related differences. Results in the BC sample were consistent with those observed in the OASIS and IXI samples, and magnitudes of explained variance on age-related differences in volume and fractal dimensionality were generally in-between those observed in each of the other data sets.

4. Discussion

When examining age-related differences in brain structure, it is important to consider the most appropriate measure. With cortical structure, it has been established that age-related differences are reflected most in cortical thickness, rather than surface area or volume (Fjell et al., 2009; Hogstrom et al., 2013; McKay et al., 2014; Salat et al., 2004); however, we recently demonstrated that structural complexity of the cortex is more sensitive to age-related differences than thickness (Madan and Kensinger, 2016). In the present study, we found systematic age-related differences in the structural complexity of subcortical regions that was not captured by volumetric measures. In addition, we found that structural complexity was not more closely related to age-related differences across all brain structures: this measure showed a weaker association with age for the ventricular regions than did other metrics. Thus, it is clear that considering the shape of subcortical structures provides additional information about age-related atrophy beyond ICV-corrected volume, but only when the "contents" of the structure are themselves meaningful—that is, neural tissue, rather than CSF.

Evidence of age-related differences in fractal dimensionality in subcortical structures (as well as cortical structures; Madan and Kensinger, 2016) demonstrates that current approaches of measuring age-related differences in volume (and cortical thickness) only partially characterize how the structural properties of

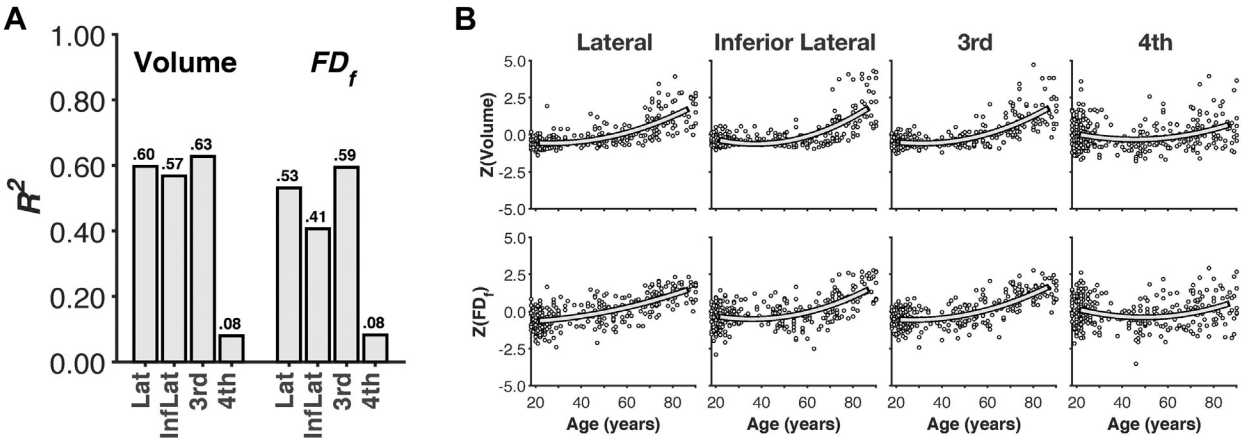

Fig. 6. Age-related differences in volume and structural complexity of ventricular structures. (A) Bar plot of amount of variance explained (R^2) by quadratic models of age. (B) Scatter plots of age-related differences in either measure.

the brain relate to age. Although the neurobiological basis (i.e., cellular through systems level) of these differences is unclear, these differences are demonstrably evident at the macro level of brain structures that is measured using structural MRIs. Further research is needed to establish how these shape-related differences manifest in more precise measures of neural structure (e.g., differences in neuronal composition or density). Indeed, the use of fractal dimensionality to measure complexity at the micro- and meso-level structures within neuroscience has already been established (Di Ieva et al., 2013, 2015) and may prove useful in examining age-related differences within these subcortical structures, such as in the composition of neurons. Nonetheless, the present results provide evidence of an additional metric for evaluating interindividual differences in physiological brain age.

Prior work in young and older adults has demonstrated that fractal dimensionality can index interindividual differences in brain morphology that relate to cognition and differs between healthy adults and patient populations. Although the current work applies fractal dimensionality analyses to subcortical structures, others have used fractal dimensionality to characterize the structural complexity of segmented gray or white matter structure (e.g., King et al., 2009; Madan and Kensinger, 2016; Mustafa et al., 2012; Sandu et al., 2008). Using these approaches, fractal dimensionality has been related to interindividual differences in measures of fluid intelligence (Mustafa et al., 2012; Sandu et al., 2014), intelligence quotient (Im et al., 2006), and performance on the cognitive subscale of the Alzheimer's Disease Assessment Scale (King et al., 2010). Fractal dimensionality has also been shown to differ between healthy adults and a number of patient populations, particularly in Alzheimer's disease (King et al., 2009, 2010; Thompson et al., 1998) and schizophrenia (Ha et al., 2005; Narr et al., 2004; Nenadic et al., 2014; Sandu et al., 2008; Yotter et al., 2011; Zhao et al., 2016). Thus, although we have demonstrated the benefits of using fractal dimensionality to index age-related differences in subcortical structure, as well as cortical structure (Madan and Kensinger, 2016), the variability of this morphologic measure also is related to interindividual differences in cognitive measures and may hold promise as a biomarker for some neurological disorders. However, it is important to consider that more interindividual variability explained by age may not always be desired, as this leaves less variance available to be related to other factors, for example, performance on cognitive measures, so volume may still be a preferable measure depending on the research question. As such, we advocate for the use of multiple brain morphology measures when examining interindividual differences.

Although we measured structural complexity here using fractal dimensionality, this is not the only approach to quantify these shape-related properties; other related approaches such as spherical harmonics (Chung et al., 2008, 2010; Yotter et al., 2011) and Laplace–Beltrami spectra (Reuter et al., 2006; Wachinger et al., 2015) may similarly be able to capture these structural differences. Seo and Chung (2011) demonstrated that Laplace–Beltrami eigenfunctions can yield better fits to the original structure than spherical harmonics, when reconstructing cortical and subcortical surfaces. This difference was attributed to Laplace–Beltrami spectra not necessitating spherical parameterization. As of yet, no comparison has been done between Laplace–Beltrami spectra and the current approach of using fractal dimensionality.

In summary, the present results reveal that metrics of fractal dimensionality can capture age-associated variance within subcortical structures that is missed when using only volumetric measures. This result represents an important extension of prior research examining cortical structure (Madan and Kensinger, 2016), revealing that fractal dimensionality is strongly associated with age even in relatively small, subcortical structures. Moreover, these results emphasize the benefits of including metrics of fractal dimensionality in assessments of structural differences associated with aging and of assessing both subcortical and cortical structures.

Disclosure statement

The authors have no conflicts of interest to disclose.

Acknowledgements

Portions of this research were supported by a grant from the National Institutes of Health (MH080833; to EAK), a fellowship from the Canadian Institutes of Health Research (FRN-146793; to CRM), and by funding provided by Boston College. MRI data used in the preparation of this article were obtained from: (1) the Open Access Series of Imaging Studies (Marcus et al., 2007); (2) the Information eXtraction from Images (IXI) dataset (funded by Engineering and Physical Sciences Research Council [EPSRC] of the UK [EPSRC GR/S21533/02]); and (3) the BC data was acquired with the support of funding from the Searle Foundation, the McKnight Foundation, and the National Institutes of Mental Health (MH080833).

References

Allen, J.S., Bruss, J., Brown, C.K., Damasio, H., 2005. Normal neuroanatomical variation due to age: the major lobes and a parcellation of the temporal region. Neurobiol. Aging 26, 1245–1260.

Apostolova, L.G., Green, A.E., Babakchanian, S., Hwang, K.S., Chou, Y.-Y., Toga, A.W., Thompson, P.M., 2012. Hippocampal atrophy and ventricular enlargement in normal aging, mild cognitive impairment (MCI), and Alzheimer disease. Alzheimer Dis. Assoc. Disord. 26, 17–27.

Barron, S.A., Jacobs, L., Kinkel, W.R., 1976. Changes in size of normal lateral ventricles during aging determined by computerized tomography. Neurology 26, 1011–1013.

Buckner, R.L., Head, D., Parker, J., Fotenos, A.F., Marcus, D., Morris, J.C., Snyder, A.Z., 2004. A unified approach for morphometric and functional data analysis in young, old, and demented adults using automated atlas-based head size normalization: reliability and validation against manual measurement of total intracranial volume. Neuroimage 23, 724–738.

Burnham, K.E., Anderson, D.R., 2002. Model Selection and Multimodel Inference, second ed. Springer-Verlag, New York.

Burnham, K.P., Anderson, D.R., 2004. Multimodel inference: understanding AIC and BIC in model selection. Sociol. Methods Res. 33, 261–304.

Caserta, F., Eldred, W.D., Fernandez, E., Hausman, R.E., Stanford, L.R., Bulderev, S.V., Schwarzer, S., Stanley, H.E., 1995. Determination of fractal dimension of physiologically characterized neurons in two and three dimensions. J. Neurosci. Methods 56, 133–144.

Chung, M.K., Nacewicz, B.M., Wang, S., Dalton, K.M., Pollak, S., Davidson, R.J., 2008. Amygdala surface modeling with weighted spherical harmonics. Lect. Notes Comput. Sci. 5128, 177–184.

Chung, M.K., Worsley, K.J., Nacewicz, B.M., Dalton, K.M., Davidson, R.J., 2010. General multivariate linear modeling of surface shapes using SurfStat. Neuroimage 53, 491–505.

Creasey, H., Rapoport, S.I., 1985. The aging human brain. Ann. Neurol. 17, 2–10.

Di Ieva, A., Esteban, F.J., Grizzi, F., Klonowski, W., Martin-Landrove, M., 2015. Fractals in the neurosciences, Part II: clinical applications and future perspectives. Neuroscientist 21, 30–43.

Di Ieva, A., Grizzi, F., Jelinek, H., Pellionisz, A.J., Losa, G.A., 2013. Fractals in the neurosciences, Part I: general principles and basic neurosciences. Neuroscientist 20, 403–417.

Drayer, B.P., 1988. Imaging of the aging brain. Part I. Normal findings. Radiology 166, 785–796.

Fischl, B., 2012. FreeSurfer. Neuroimage 62, 774–781.

Fischl, B., Dale, A.M., 2000. Measuring the thickness of the human cerebral cortex from magnetic resonance images. Proc. Natl. Acad. Sci. U. S. A. 97, 11050–11055.

Fischl, B., Salat, D.H., Busa, E., Albert, M., Dieterich, M., Haselgrove, C., van der Kouwe, A., Killiany, R., Kennedy, D., Klaveness, S., Montillo, A., Makris, N., Rosen, B., Dale, A.M., 2002. Whole brain segmentation: automated labelling of neuroanatomical structures in the human brain. Neuron 33, 341–355.

Fischl, B., Salat, D.H., van der Kouwe, A.J.W., Makris, N., Ségonne, F., Quinn, B.T., Dale, A.M., 2004. Sequence-independent segmentation of magnetic resonance images. Neuroimage 23, S69–S84.

Fischl, B., Sereno, M.I., Dale, A.M., 1999. Cortical surface-based analysis. Neuroimage 9, 195–207.

Fjell, A.M., Westlye, L.T., Amlien, I., Espeseth, T., Reinvang, I., Raz, N., Agartz, I., Salat, D.H., Greve, D.N., Fischl, B., Dale, A.M., Walhovd, K.B., 2009. High consistency of regional cortical thinning in aging across multiple samples. Cereb. Cortex 19, 2001–2012.

Free, S.L., Sisodiya, S.M., Cook, M.J., Fish, D.R., Shorvon, S.D., 1996. Three-dimensional fractal analysis of the white matter surface from magnetic resonance images of the human brain. Cereb. Cortex 6, 830–836.

Goodro, M., Sameti, M., Patenaude, B., Fein, G., 2012. Age effect on subcortical structures in healthy adults. Psychiatry Res. 203, 38–45.

Greenberg, D.L., Messer, D.F., Payne, M.E., MacFall, J.R., Provenzale, J.M., Steffens, D.C., Krishnan, R.R., 2008. Aging, gender, and the elderly adult brain: an examination of analytical strategies. Neurobiol. Aging 29, 290–302.

Gunning-Dixon, F.M., Head, D., McQuain, J., Acker, J.D., Raz, N., 1998. Differential aging of the human striatum: a prospective MR imaging study. Am. J. Neuroradiol. 19, 1501–1507.

Ha, T.H., Yoon, U., Lee, K.J., Shin, Y.W., Lee, J.-M., Kim, I.Y., Ha, K.S., Kim, S.I., Kwon, J.S., 2005. Fractal dimension of cerebral cortical surface in schizophrenia and obsessive–compulsive disorder. Neurosci. Lett. 384, 172–176.

Hogstrom, L.J., Westlye, L.T., Walhovd, K.B., Fjell, A.M., 2013. The structure of the cerebral cortex across adult life: age-related patterns of surface area, thickness, and gyrification. Cereb. Cortex 23, 2521–2530.

Hofman, M.A., 1991. The fractal geometry of convoluted brains. J. Hirnforsch. 32, 103–111.

Hrybouski, S., Aghamohammadi-Sereshki, A., Madan, C.R., Shafer, A.T., Baron, C.A., Seres, P., Beaulieu, C., Olsen, F., Malykhin, N.V., 2016. Amygdala subnuclei response and connectivity during emotional processing. Neuroimage 133, 98–110.

Im, K., Lee, J.-M., Yoon, U., Shin, Y.-W., Hong, S.B., Kim, I.Y., Kwon, J.S., Kim, S.I., 2006. Fractal dimension in human cortical surface: multiple regression analysis with cortical thickness, sulcal depth, and folding area. Hum. Brain Mapp. 27, 994–1003.

Inano, S., Takao, H., Hayashi, N., Yoshioka, N., Mori, H., Kunimatsu, A., Abe, O., Ohtomo, K., 2013. Effects of age and gender on neuroanatomical volumes. J. Magn. Reson. Imaging 37, 1072–1076.

Jernigan, T.L., Archibald, S.L., Fennema-Notestine, C., Gamst, A.C., Stout, J.C., Bonner, J., Hesselink, J.R., 2001. Effects of age on tissues and regions of the cerebrum and cerebellum. Neurobiol. Aging 22, 581–594.

Jovicich, J., Czanner, S., Han, X., Salat, D.H., van der Kouwe, A.J.W., Quinn, B., Pacheco, J., Albert, M., Killany, R., Blacker, D., Maguire, P., Rosas, D., Makris, N., Gollub, R., Dale, A.M., Dickerson, B.C., Fischl, B., 2009. MRI-derived measurements of human subcortical, ventricular and intracranial brain volumes: reliability effects of scan sessions, acquisition sequences, data analyses, scanner upgrade, scanner vendors and field strengths. Neuroimage 46, 177–192.

Kaye, J.A., DeCarli, C., Luxenberg, J.S., Rapoport, S.I., 1992. The significance of age-related enlargement of the cerebral ventricles in healthy men and women measured by quantitative computed X-ray tomography. J. Am. Geriatr. Soc. 40, 225–231.

Keller, S.S., Gerdes, J.S., Mohammadi, S., Kellinghaus, C., Kugel, H., Deppe, K., Ringelstein, E.B., Evers, S., Schwindt, W., Deppe, M., 2012. Volume estimation of the thalamus using FreeSurfer and stereology: consistency between methods. Neuroinformatics 10, 341–350.

Kemper, T.L., 1994. Neuroanatomical and neuropathological changes during aging and dementia. In: Albert, M.L., Knoefel, J.E. (Eds.), Clinical Neurology of Aging, second ed. Oxford University Press, New York, pp. 3–67.

King, R.D., Brown, B., Hwang, M., Jeon, T., George, A.T., 2010. Fractal dimension analysis of the cortical ribbon in mild Alzheimer's disease. Neuroimage 53, 471–479.

King, R.D., George, A.T., Jeon, T., Hynan, L.S., Youn, T.S., Kennedy, D.N., Dickerson, B., 2009. Characterization of atrophic changes in the cerebral cortex using fractal dimensional analysis. Brain Imaging Behav. 3, 154–166.

Kiselev, V.G., Hahn, K.R., Auer, D.P., 2003. Is the brain cortex a fractal? Neuroimage 20, 1765–1774.

Kochunov, P., Thompson, P.M., Coyle, T.R., Lancaster, J.L., Kochunov, V., Royall, D., Mangin, J.-F., Rivière, D., Fox, P.T., 2008. Relationship among neuroimaging indices of cerebral health during normal aging. Hum. Brain Mapp. 29, 36–45.

La Joie, R., Fouquet, M., Mézenge, F., Landeau, B., Villain, N., Mevel, K., Pélerin, A., Eustache, F., Desgranges, B., Chételat, G., 2010. Differential effect of age on hippocampal subfields assessed using a new high-resolution 3T MR sequence. Neuroimage 53, 506–514.

Lehmann, M., Douiri, A., Kim, L.G., Modat, M., Chan, D., Ourselin, S., Barnes, J., Fox, N.C., 2010. Atrophy patterns in Alzheimer's disease and semantic dementia: a comparison of FreeSurfer and manual volumetric measurements. Neuroimage 49, 2264–2274.

LeMay, M., 1984. Radiologic changes of the aging brain and skull. Am. J. Roentgenol. 143, 383–389.

Long, X., Liao, W., Jiang, C., Liang, D., Qiu, B., Zhang, L., 2012. Healthy aging: an automatic analysis of global and regional morphological alterations of human brain. Acad. Radiol. 19, 785–793.

Madan, C.R., 2015. Creating 3D visualizations of MRI data: a brief guide. F1000Res. 4, 466.

Madan, C.R., Kensinger, E.A., 2016. Cortical complexity as a measure of age-related brain atrophy. Neuroimage 134, 617–629.

Mandelbrot, B.B., 1967. How long is the coast of Britain? Statistical self-similarity and fractional dimension. Science 156, 636–638.

Mandelbrot, B.B., 1982. The Fractal Geometry of Nature. W.H. Freeman, San Francisco.

Marcus, D.S., Wang, T.H., Parker, J., Csernansky, J.G., Morris, J.C., Buckner, R.L., 2007. Open Access Series of Imaging Studies (OASIS): cross-sectional MRI Data in young, middle aged, nondemented, and demented older adults. J. Cogn. Neurosci. 19, 1498–1507.

McKay, D.R., Knowles, E.E.M., Winkler, A.A.M., Sprooten, E., Kochunov, P., Olvera, R.L., Curran, J.E., Kent Jr, J.W., Carless, M.A., Göring, H.H., Dyer, T.D., Duggirala, R., Almasy, L., Fox, P.T., Blangero, J., Glahn, D.C., 2014. Influence of age, sex and genetic factors on the human brain. Brain Imaging Behav. 8, 143–152.

Mulder, E.R., de Jong, R.A., Knol, D.L., van Schijndel, R.A., Cover, K.S., Visser, P.J., Barkhof, F., Vrenken, H. Alzheimer's Disease Neuroimaging Initiative, 2014. Hippocampal volume change measurement: quantitative assessment of the reproducibility of expert manual outlining and the automated methods FreeSurfer and FIRST. Neuroimage 92, 169–181.

Mustafa, N., Ahearn, T.S., Waiter, G.D., Murray, A.D., Whalley, L.J., Staff, R.T., 2012. Brain structural complexity and life course cognitive change. Neuroimage 61, 694–701.

Narr, K.L., Bilder, R.M., Kim, S., Thompson, P.M., Szeszko, P., Robinson, D., Luders, E., Toga, A.W., 2004. Abnormal gyral complexity in first-episode schizophrenia. Biol. Psychiatry 55, 859–867.

Nenadic, I., Yotter, R.A., Sauer, H., Gaser, C., 2014. Cortical surface complexity in frontal and temporal areas varies across subgroups of schizophrenia. Hum. Brain Mapp. 35, 1691–1699.

Nestor, S.M., Rupsingh, R., Borrie, M., Smith, M., Accomazzi, V., Wells, J.L., Fogarty, J., Bartha, R., 2008. Ventricular enlargement as a possible measure of Alzheimer's disease progression validated using the Alzheimer's disease neuroimaging initiative database. Brain 131, 2443–2454.

Palombo, D.J., Amaral, R.S.C., Olsen, R.K., Muller, D.J., Todd, R.M., Anderson, A.K., Levine, B., 2013. KIBRA polymorphism is associated with individual differences in Hippocampal subregions: evidence from anatomical segmentation using high-resolution MRI. J. Neurosci. 33, 13088–13093.

Pardoe H, R., Pell, G.S., Abbott, D.F., Jackson, G.D., 2009. Hippocampal volume assessment in temporal lobe epilepsy: How good is automated segmentation? Epilepsia 50, 2586–2592.
Pienaar, R., Fischl, B., Caviness, V., Makris, N., Grant, P.E., 2008. A methodology for analyzing curvature in the developing brain from preterm to adult. Int. J. Imaging Syst. Technol. 18, 42–68.
Potvin, O., Mouiha, A., Dieumegarde, L., Duchesne, S., 2016. Normative data for subcortical regional volumes over the lifetime of the adult human brain. Neuroimage 137, 9–20.
Qiu, A., Zhong, J., Graham, S., Chia, M.Y., Sim, K., 2009. Combined analyses of thalamic volume, shape and white matter integrity in first-episode schizophrenia. Neuroimage 47, 1163–1171.
Raz, N., Lindenberger, U., Rodrigue, K.M., Kennedy, K.M., Head, D., Williamson, A., Dahle, C., Gerstorf, D., Acker, J.D., 2005. Regional brain changes in aging healthy adults: general trends, individual differences and modifiers. Cereb. Cortex 15, 1676–1689.
Raz, N., Rodrigue, K.M., 2006. Differential aging of the brain: patterns, cognitive correlates and modifiers. Neurosci. Biobehav. Rev. 30, 730–748.
Raz, N., Rodrigue, K.M., Head, D., Kennedy, K.M., Acker, J.D., 2004. Differential aging of the medial temporal lobe: a study of a five-year change. Neurology 62, 433–438.
Reagh, Z.M., Yassa, M.A., 2014. Object and spatial mnemonic interference differentially engage lateral and medial entorhinal cortex in humans. Proc. Natl. Acad. Sci. U. S. A. 111, E4264–E4273.
Reuter, M., Wolter, F.-E., Peinecke, N., 2006. Laplace–Beltrami spectra as "Shape-DNA" of surfaces and solids. Comput. Aided Des. 38, 342–366.
Salat, D.H., Buckner, R.L., Snyder, A.Z., Greve, D.N., Desikan, R.S., Busa, E., Morris, J.C., Dale, A.M., Fischl, B., 2004. Thinning of the cerebral cortex in aging. Cereb. Cortex 14, 721–730.
Sandu, A.-L., Rasmussen, I.-A., Lundervold, A., Kreuder, F., Neckelmann, G., Hugdahl, K., Specht, K., 2008. Fractal dimension analysis of MR images reveals grey matter structure irregularities in schizophrenia. Comput. Med. Imaging Graph. 32, 150–158.
Sandu, A.-L., Staff, R.T., McNeil, C.J., Mustafa, N., Ahearn, T., Whalley, L.J., Murray, A.D., 2014. Structural brain complexity and cognitive decline in late life: a longitudinal study in the Aberdeen 1936 Birth Cohort. Neuroimage 100, 558–563.
Sargolzaei, S., Sargolzaei, A., Cabrerizo, M., Chen, G., Goryawala, M., Pinzon-Ardila, A., Gonzalez-Arias, S.M., Adjouadi, M., 2015. Estimating intracranial volume in brain research: an evaluation of methods. Neuroinformatics 13, 427–441.
Seo, S., Chung, M.K., 2011. Laplace-Beltrami eigenfunction expansion of cortical manifolds. IEEE Int. Symp. Biomed. Imaging 2011, 372–375.
Smith, M.J., Wang, L., Cronenwett, W., Goldman, M.B., Mamah, D., Barch, D.M., Csernansky, J.G., 2011. Alcohol use disorders contribute to hippocampal and subcortical shape differences in schizophrenia. Schizophr. Res. 131, 174–183.
Tae, W.S., Kim, S.S., Lee, K.U., Nam, E.-C., Kim, K.W., 2008. Validation of hippocampal volumes measured using a manual method and two automated methods (FreeSurfer and IBASPM) in chronic major depressive disorder. Neuroradiology 50, 569–581.
Tamnes, C.K., Walhovd, K.B., Dale, A.M., Østby, Y., Grydeland, H., Richardson, G., Westlye, L.T., Roddey, J.C., Hagler Jr, D.J., Due-Tønnessen, P., Holland, D., Fjell, A.M. Alzheimer's Disease Neuroimaging Initiative, 2013. Brain development and aging: overlapping and unique patterns of change. Neuroimage 68, 63–74.
Tang, X., Holland, D., Dale, A.M., Younes, L., Miller, M.I., 2014. Shape abnormalities of subcortical and ventricular structures in mild cognitive impairment and Alzheimer's disease: detecting, quantifying, and predicting. Hum. Brain Mapp. 35, 3701–3725.
Thompson, P., Moussai, J., Zohoori, A., Khan, A.A., Mega, M.S., Cummings, J.L., Toga, A.W., 1998. Cortical variability and asymmetry in normal aging and Alzheimer's disease. Cereb. Cortex 8, 492–509.
Thompson, P.M., Schwartz, C., Lin, R.T., Khan, A.A., Toga, A.W., 1996. Three-dimensional statistical analysis of sulcal variability in the human brain. J. Neurosci. 16, 4261–4274.
Toro, R., Poline, J.-B., Huguet, G., Loth, E., Frouin, V., Banaschewski, T., Barker, G.J., Bokde, A., Büchel, C., Carvalho, F.M., Conrod, P., Fauth-Bühler, M., Flor, H., Gallinat, J., Garavan, H., Gowland, P., Heinz, A., Ittermann, B., Lawrence, C., Lemaître, H., Mann, K., Nees, F., Paus, T., Pausova, Z., Rietschel, M., Robbins, T., Smolka, M.N., Ströhle, A., Schumann, G., Bourgeron, T. IMAGEN Consortium, 2014. Genomic architecture of human neuroanatomical diversity. Mol. Psychiatry 20, 1011–1016.
van der Kouwe, A.J.W., Benner, T., Salat, D.H., Fischl, B., 2008. Brain morphometry with multiecho MPRAGE. Neuroimage 40, 559–569.
Wachinger, C., Golland, P., Kremen, W., Fischl, B., Reuter, M., 2015. BrainPrint: a discriminative characterization of brain morphology. Neuroimage 109, 232–248.
Walhovd, K.B., Fjell, A.M., Reinvang, I., Lundervold, A., Dale, A.M., Eilertsen, D.E., Quinn, B.T., Salat, D., Makris, N., Fischl, B., 2005. Effects of age on volumes of cortex, white matter and subcortical structures. Neurobiol. Aging 26, 1261–1270.
Walhovd, K.B., Westlye, L.T., Amlien, I., Espeseth, T., Reinvang, I., Raz, N., Agartz, I., Salat, D.H., Greve, D.N., Fischl, B., Dale, A.M., Fjell, A.M., 2011. Consistent neuroanatomical age-related volume differences across multiple samples. Neurobiol. Aging 32, 916–932.
Wenger, E., Mårtensson, J., Noack, H., Bodammer, N.C., Kühn, S., Schaefer, S., Heinze, H.J., Düzel, E., Bäckman, L., Lindenberger, U., Lövdén, M., 2014. Comparing manual and automatic segmentation of hippocampal volumes: reliability and validity issues in younger and older brains. Hum. Brain Mapp. 35, 4236–4248.
Wonderlick, J.S., Ziegler, D.A., Hosseini-Varnamkhasti, P., Locascio, J.J., Bakkour, A., van der Kouwe, A., Triantafyllou, C., Corkin, S., Dickerson, B.C., 2009. Reliability of MRI-derived cortical and subcortical morphometric measures: effects of pulse sequence, voxel geometry, and parallel imaging. Neuroimage 44, 1324–1333.
Yang, Z., Wen, W., Jiang, J., Crawford, J.D., Reppermund, S., Levitan, C., Slavin, M.J., Kochan, N.A., Richmond, R.L., Brodaty, H., Trollor, J.N., Sachdev, P.S., 2016. Age-associated differences on structural brain MRI in nondemented individuals from 71 to 103 years. Neurobiol. Aging 40, 86–97.
Yotter, R.A., Nenadic, I., Ziegler, G., Thompson, P.M., Gaser, C., 2011. Local cortical surface complexity maps from spherical harmonic reconstructions. Neuroimage 56, 961–973.
Yun, H.J., Im, K., Yang, Jin-Ju, Yoon, U., Lee, J.-M., 2013. Automated sulcal depth measurement on cortical surface reflecting geometrical properties of sulci. PLoS One 8, e55977.
Yushkevich, P.A., Pluta, J.B., Wang, H., Xie, L., Ding, S.-L., Gertje, E.C., Mancuso, L., Kliot, D., Das, S.R., Wolk, D.A., 2015. Automated volumetry and regional thickness analysis of hippocampal subfields and medial temporal cortical structures in mild cognitive impairment. Hum. Brain Mapp. 36, 258–287.
Zhao, G., Denisova, K., Sehatpour, P., Long, J., Gui, W., Qiao, J., Javitt, D.C., Wang, Z., 2016. Fractal dimension analysis of subcortical gray matter structures in Schizophrenia. PLoS One 11, e0155415.